ChemComm

Accepted Manuscript

This article can be cited before page numbers have been issued, to do this please use: B. Kaur, K. Malecka, C. S. Chay, D. A. Cristaldi, I. Mames, H. Radecka, J. Radecki and E. Stulz, *Chem. Commun.*, 2018, DOI: 10.1039/C8CC05362F.

ROYAL SOCIETY OF CHEMISTRY

rsc.li/chemcomm

View Article Online
DOI: 10.1039/C8CC05362F

ChemComm

COMMUNICATION

Approaching single DNA molecule detection with an ultrasensitive electrochemical genosensor based on gold nanoparticles and Cobalt-porphyrin DNA conjugates

Received 00th January 20xx,
Accepted 00th January 20xx

DOI: 10.1039/x0xx00000x

www.rsc.org/

Balwinder Kaur,[†a] Kamila Malecka,[†a] Domenico A. Cristaldi,[†b] Clarissa S. Chay,[†b] Iwona Mames,[†b] Hanna Radecka,[a] Jerzy Radecki*[a] and Eugen Stulz*[b]

We describe an ultrasensitive electrochemical genosensor based on gold nanoparticles and cobalt-porphyrin functionalised ssDNA probes. The sensitivity at the attomolar concentration level arises from an increased density of redox labels on the electrode surface compared to sensors without NP modification. The electrode detects as few as 23 DNA molecules, approaching single molecule detection.

There is currently a great interest in highly sensitive DNA biosensors due to increased risks and threats from pathogens, but also for early diagnostics of gene associated diseases such as cancer.[1] The genosensors find widespread use in clinical diagnosis, pathogen detection, DNA sequencing and mapping, and in forensics.[2] In particular, the detection of single nucleotide polymorphism (SNP) is of high importance in specific allele analysis, which can indicate susceptibility for specific diseases.[3]

Generally, in genosensors the hybridisation process between the ssDNA probe and its complementary target is converted into a readable signal by appropriate transducers like electrochemical, optical or mass-sensitive elements. Among the different sensing methods, electrochemical detection offers one of the best options for DNA sensing due to its simplicity, fast response, low cost, ease of miniaturization and potential for multiplexing in microfluidic chips.[4] To date a variety of electrochemical genosensors for specific ssDNA sequence detection have been reported in the literature.[5] These genosensors are based either on direct oxidation or reduction of nucleic acids, on electrodes modified with label-free ssDNA probe and diffusional redox markers such as $Fe[(CN)_6]^{3-/4-}$, or $[Ru(NH_3)_6]^{3+}$ in the sample solution. The sensors which incorporate a ssDNA probe labelled with redox markers, such as methylene blue or ferrocene, are often called signal-on or signal-off DNA sensors, depending on their design.[2b, 2d]

Improving the sensitivity and detection limit are two of the major challenges in the preparation of genosensors, and particularly the amount of immobilised ssDNA probe on the biosensor interface further determines its recognition capability towards complementary ssDNA. In order to increase the immobilisation amount of the ssDNA probe and improve its hybridisation efficiency, different nanomaterials have been investigated for electrode surface modification to increase their surface areas.[6] In recent years, DNA genosensors based on metal nanoparticles (Pt, Au and Ag) for signal amplification have been developed with substantial improvement in sensitivity.[7] DNA-gold nanoparticle conjugates have been explored as one of the most attractive nanomaterials because of their unique chemical and physical properties and ease of formation.[7d, 7e, 8] The reported sensors with nanoparticle modification generally exhibit detection limits (LODs) in the range of 10^{-9} to 10^{-15} M;[7e, 8a, 8b, 9] one report describes a LOD of 1.7×10^{-18} M where a AuNP was attached to the end of a hairpin loop and acts as mediator for the $[Fe(CN)_6]^{3-/4-}$ redox couple detection.[10]

Here we report a new strategy to prepare DNA biosensors based on gold nanoparticles (AuNPs) combined with cobalt-porphyrin (CoP) labelled ssDNA probes,[11] which are immobilized on the gold electrode surface. The CoP acts as redox marker for the sensitive detection of the target ssDNA derived from Avian Influenza Virus (AIV); this marker has previously shown to be very sensitive and selective, allowing efficiently discrimination of single base pair mismatches in the femtomolar range and does not require an externally added redox mediator, which is a great advantage.[11a] AIV, especially the type H5N1, is a highly contagious, poultry threatening pathogen which can also infect humans. Thus, there is a requirement for highly sensitive, accurate and rapid tests for diagnosis of AIV infection which would allow early antiviral therapy.[12] In recent years, our laboratories have developed DNA biosensors towards the detection of H5N1.[2b, 11a, 13] Using

[a] Institute of Animal Reproduction and Food Research, Polish Academy of Sciences, Tuwima 10, 10-748 Olsztyn, Poland, E-mail: j.radecki@pan.olsztyn.pl.
[b] School of Chemistry & Institute for Life Sciences, University of Southampton, Highfield, Southampton SO17 1BJ, UK, E-mail: est@soton.ac.uk.
† These authors contributed equally to the work.
Electronic Supplementary Information (ESI) available: synthesis and full characterisation of the DNA-NP conjugates and of the electrochemical sensor. See DOI: 10.1039/x0xx00000x

View Article Online
DOI: 10.1039/C8CC05362F

AuNPs, an increase of ssDNA probe molecules and with it the number of redox centres responsible for the analytical signal generation was achieved on an electrode, resulting in a genosensor with greatly improved sensitivity. A detailed study to determine the effect of AuNPs surface functionalization with different amounts of CoP-ssDNA on the detection of DNA targets is presented.

The steps in the genosensor fabrication and the working principle are depicted in Scheme 1 (details of the procedures can be found in the electronic supporting information). The first step involves modification of the gold electrode surface with a thiol-DNA capture strand, which is complementary to the CoP-ssDNA probe; the capture strand is embedded in a self-assembled monolayer (SAM) of mercaptohexanol (MCH). In a separate step, AuNPs (13 nm, Fig. S4) were functionalised with CoP-DNA (probe strand)[11b] through covalent Au-thiol bonding; as in our previous sensor, three dithiol serinol units at the 5'-end were used to ensure stability of the conjugate.[11a] Different ratios of AuNPs to ssDNA at 1:10, 1:100 and 1:200 were used (by virtue of concentration); no MCH filler was used on the NPs. The AuNP–CoP-ssDNA conjugates were then attached to the gold electrode surface *via* hybridisation of the two complementary strands. In this respect, some of the ssDNA probe is used to bind the NPs to the gold surface and burying this amount of the porphyrin markers; however, since not all probe strands are used in this process it leaves enough CoP-ssDNA strands for capturing the target strands in solution.

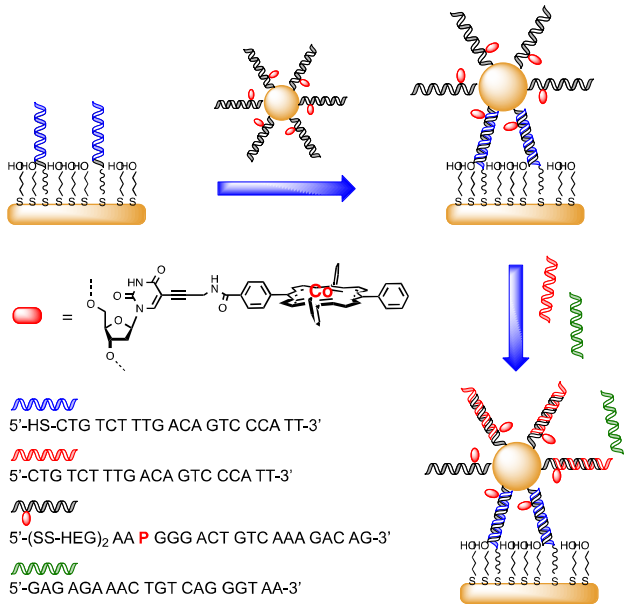

Scheme 1. Schematic representation of the genosensor fabrication. The blue capture strand is attached via single thiol modification; the black probe strand containing the porphyrin (**P**) is anchored by two repeating disulfide and hexaethylene glycol spacer units (see ESI).

To visualise the adsorption of the modified AuNPs onto the substrate, AFM images were recorded using a gold layered mica substrate which was prepared in an identical way to the electrodes. The images were recorded using non-contact mode in air, and representative images are shown in Fig. 1a. The bare gold surface shows a high degree of structural homogeneity with well-defined terraces and a root mean squared (RMS) roughness of 3.27 ± 0.17 nm, which was determined over an area of 0.50 μm^2. The topography of the AuNP modified gold surface is shown in Fig. 1b, and well separated NPs are visible. The RMS roughness, determined over the same area as before, was equal to 7.49 ± 0.45 nm. The size of the observed AuNPs was found to be 46.6 ± 1.7 nm, which is larger than the AuNPs themselves (13 nm). Similar size increase in AuNP-DNA conjugates with a comparable DNA length (from 17 nm NP to 69.8 nm NP-DNA conjugate with an 18 bp DNA) have been reported,[14] therefore the increase can be accounted for by the ssDNA layer. The dispersion of the NPs on the gold surface also indicates that no aggregation occurs, which would show substantially larger sizes.[14]

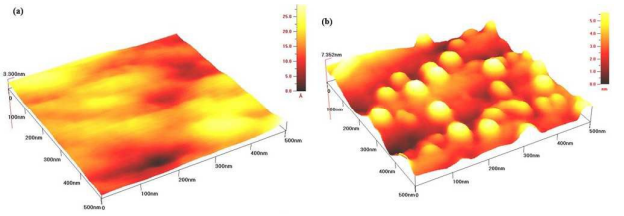

Figure 1. AFM images of: (a) Au(111) thin film on mica substrate and (b) Au(111) substrate modified with SH-ssDNA+MCH/AuNPs-CoP-ssDNA (1:200).

The functional electrode was next fully characterised using electrochemical methods. The presence of the redox active probe (CoP) on the electrode surface was confirmed by cyclic voltammetry (CV), Osteryoung square wave voltammetry (OSWV) and differential pulse voltammetry (DPV). Representative voltammograms for all systems are shown in Fig. S6 (supporting information). The gold electrodes, which were modified with AuNPs-CoP–ssDNA using 1:10, 1:100 and 1:200 ratio, all exhibited well defined quasi-reversible Co(II)/Co(III) redox peaks. The electrochemical parameters (peak positions and peak current values) obtained for this study are summarised in Table S1, and the redox potentials generally centre around +300 mV. The Co(II)/Co(III) redox peaks are also clearly visible in the representative OSWV (Fig. S6b), and DPV confirmed well-defined oxidation Co(II)/Co(III) and reduction Co(III)/Co(II) peaks for the redox processes (Fig. S6c,d). The current intensity as well as the peak potential for the Co(II)/Co(III) redox process resulted in the same potential position for all systems studied (Table S1) and does not vary greatly for the different loadings. Therefore, the sensors show good consistency in their redox behaviour.

To confirm that the redox centres are located at the electrode surface, the effect of the scan rate on the peak currents was investigated. Fig. S7 shows that all systems exhibit a linear relationship between the scan rate and the anodic or cathodic peak currents. This indicates that the redox process is not diffusion controlled and the redox centres are indeed located on the surface of the gold electrode. The relationship between scan rate *vs* anodic and cathodic peak currents was used to calculate the density of redox active layer (Γ). The density Γ for

View Article Online
DOI: 10.1039/C8CC05362F

all systems was found to be similar at around 2.9 × 10^{-11} mol/cm^2 (Table S2), which is a factor of 2.5 higher than without NPs.[11a] In addition, the data presented in Fig. S7 also confirms that the anodic peak shifts towards positive potential values, whereas the cathodic peak shifts in the direction of negative potential with increasing scan rate. Electrochemical parameters such as the electron transfer coefficient (α) and the electrode reaction standard rate constant (k_s) were calculated from the relationship between the natural logarithm of the scan rate *vs* the anodic or cathodic peak potential using Laviron's equation (Table S2).[15] The electron transfer coefficient values calculated for the modified gold electrodes are very similar in the range of α = 0.66 – 0.74. For all systems, and similar values of k_s = 0.7 s^{-1} were observed.

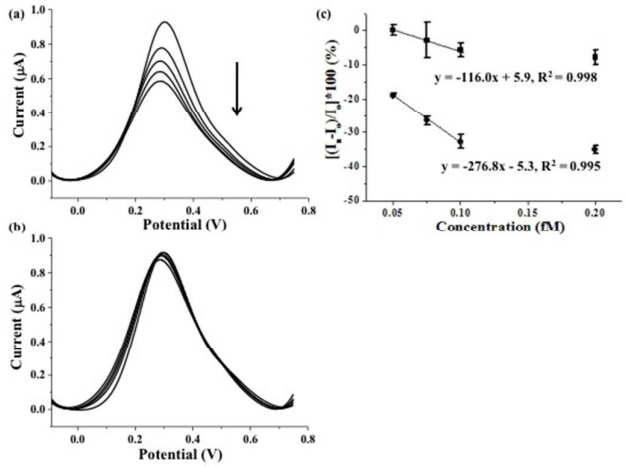

Figure 2. Representative Osteryoung square-wave voltammograms recorded using gold electrodes modified with SH-ssDNA+MCH/AuNPs-CoP-ssDNA (1:200) upon hybridization with 20-mer (a) c-ssDNA (complementary) and (b) nc-ssDNA (non-complementary) at concentrations (i) 0, (ii) 0.05, (iii) 0.075, (iv) 0.1 and (v) 0.2 fM (buffer composition: 2.5 mM NaH_2PO_4, 2.5 mM Na_2HPO_4 and 50 mM NaCl, pH 7.0). (c) Relative intensity of redox couple Co(II)/Co(III) current vs. concentration of (●) c-ssDNA and (■) nc-ssDNA.

Overall, the data suggest that a similar number of CoP redox centres are "seen" on the electrode surface, irrespective of the original loading of the AuNPs with the CoP–DNA. We determined that the saturation loading of ssDNA on the AuNP is around 160 molecules per AuNP (see ESI, Fig. S5), therefore the 1:200 system should represent a fully covered AuNP, whereas at lower ratios the AuNPs are expected to be loaded with fewer redox centres. Since the AuNPs show some variation in size, the saturation number represents an average value, and we will refer to this system still as 1:200, acknowledging that some deviation from this number is present. The reduced loading in the lower ratios is clearly visible in the hybridisation tests (*vide infra*), even though it may not be reflected in the characterisation of the ssDNA electrode.

Before applying the genosensors for the detection of target ssDNA, one of the important parameters, namely the hybridisation time between the target ssDNA and ssDNA probe required for maximum target detection, was optimized (Fig. S8). The maximum decrease in the current intensity was obtained after 2 h of hybridisation time; the decrease in current corresponds perfectly to what we had observed in our sensor without NP modification and is indicative of the hybridisation event.[11a] Therefore, a hybridisation time of 2 h was used for all further experiments involving complementary as well as non-complementary ssDNA. In addition, before starting each experiment the stability of the DNA biosensor was checked by adding pure PB buffer solution and equilibrated for 2 h on the modified gold electrodes surfaces. The current responses were then measured using OSWV. Based on the obtained results it can be confidently stated that all systems are stable with a relative standard deviation (RSD) of less than 5%.

The electrodes were applied for the detection of fully complementary (c-ssDNA) and non-complementary (nc-ssDNA) sequences to the ssDNA probe using OSWV which eliminates the capacitive current. Representative OSWV curves registered after incubation with the 20-mer complementary c-ssDNA with the various modified gold electrodes are shown in Fig. 2a, Fig. S9a and Fig. S10a. The addition of target c-ssDNA produced a decrease in the Co(II)/Co(III) faradic current for all of the modified gold electrodes, as described previously.[11a] The decrease in the current is proportional to the concentration of the c-ssDNA. The non-complementary nc-ssDNA induced much smaller changes in the current (Fig. 2b, Fig. S9b and Fig. S10b). A linear range was obtained from 5.0 × 10^{-17} – 1.0 × 10^{-16} M for all gold electrodes (Fig. 2c, Fig. S9c and Fig. S10c, Table S3). The ratio of the slopes of the linear regressions of c-DNA and nc-DNA gives the response ratio $R_{i,j}$ and is a measure for the selectivity of the electrode;[16] for 1:100 and 1:200 this is 0.50 and 0.43, respectively, and indicates very good selectivity, whereas for 1:10 the ratio of 1.13 indicates poor selectivity.

The detection limits (LODs) were calculated using IUPAC definitions and applying equation (1):[17]

$$\text{LOD} = 3.3\,\sigma/q \qquad (1)$$

where σ is the standard deviation of the response and q is the slope of the calibration curve. The limit of detections for the sensors at ratio 1:10, 1:100 and 1:200 were found to be 4.8 × 10^{-17} M, 2.6 × 10^{-17} M, and 3.8 × 10^{-18} M, respectively; this is directly correlated with the relative number and density of the CoP-DNA probe on the AuNP surface. This shows that saturating the AuNPs with the CoP-DNA probe gives the sensor with the highest sensitivity and lowest LOD, while lower loadings yield LODs which are a factor of 10 less sensitive. Compared to the electrodes without AuNPs, which have a LOD of 21 fM,[11a] the decrease in LOD to 3.8 aM means a gain factor of >1000.

Given that for the incubation we used 10 µl of the target ssDNA solution, the effective detection limit of ssDNA at ratio 1:10, 1:100 and 1:200 is 4.8×10^{-22}, 2.6×10^{-22} and 3.8×10^{-23} mol and amounts to 290, 160 and 23 DNA molecules, respectively, thus approaching single molecule detection of complementary DNA. The electrode has a surface area of 0.0314 cm^2 and contains about 1.75×10^{13} detectable CoP-ssDNA molecules for

View Article Online
DOI: 10.1039/C8CC05362F

each sample (1:10, 1:100 and 1:200). A comparison with systems reported in the literature (Table S3) shows that our approach is superior to most reported sensors in terms of LOD, apart from the sensor by Li et al.[10] who reported a LOD of 1.7 aM. However, their system involved attachment of the AuNP to the end of a hairpin loop, which is removed from the electrode surface upon target binding and hairpin loop opening; no information is given on the effective numbers of detected DNA molecules.

In summary, we demonstrate that a stable genosensor can be prepared which shows a greatly improved LOD for complementary ssDNA strands by inclusion of AuNPs on the electrode surface. The use of the probe strand to both capture the AuNPs onto the surface as well as for the detection of the target ssDNA simplifies the system greatly. This avoids the use of either different DNA strands for the two purposes or using more elaborate systems such as based on biotin–streptavidin binding. The data suggest that the system improvements are primarily due to an increased number of redox markers close to the electrode surface, and no evidence of electron transfer through the nanoparticles could be observed. This system could very well be implemented in multiplexing devices, including those based on microfluidic setup, and thus be adapted to a variety of different target DNA sequences such as for viral infections, cancer or inherited genetic disorders, where rapid detection and high sensitivity are of highest importance.

This research was performed within statutory funds of Biosensors Department Institute of Animal Reproduction and Food Research, Polish Academy of Sciences, and from the University of Southampton, UK. Funding from the European Union for IM in form of a Marie Skłodowska-Curie Fellowship "Nano-DNA" (FP7-PEOPLE-2012-IEF, No 331952) is greatly acknowledged.

Conflicts of interest

There are no conflicts to declare.

Notes and references

1. (a) J.-H. Oh and J.-S. Lee, *Anal. Chem.*, 2011, **83**, 7364-7370; (b) J. Lou, Z. Wang, X. Wang, J. Bao, W. Tu and Z. Dai, *Chem. Commun.*, 2015, **51**, 14578-14581; (c) X. Chen, Y.-H. Lin, J. Li, L.-S. Lin, G.-N. Chen and H.-H. Yang, *Chem. Commun.*, 2011, **47**, 12116-12118; (d) Q. Wang, L. Yang, X. Yang, K. Wang, L. He, J. Zhu and T. Su, *Chem. Commun.*, 2012, **48**, 2982-2984.
2. (a) D. O. Ariksoysal, H. Karadeniz, A. Erdem, A. Sengonul, A. A. Sayiner and M. Ozsoz, *Anal. Chem.*, 2005, **77**, 4908-4917; (b) I. Grabowska, K. Malecka, A. Stachyra, A. Góra-Sochacka, A. Sirko, W. Zagórski-Ostoja, H. Radecka and J. Radecki, *Anal. Chem.*, 2013, **85**, 10167-10173; (c) S. Moura-Melo, R. Miranda-Castro, N. de-los-Santos-Álvarez, A. J. Miranda-Ordieres, J. R. Dos Santos Junior, R. A. da Silva Fonseca and M. J. Lobo-Castañón, *Anal. Chem.*, 2015, **87**, 8547-8554; (d) E. Farjami, L. Clima, K. Gothelf and E. E. Ferapontova, *Anal. Chem.*, 2011, **83**, 1594-1602.
3. D. Ozkan, A. Erdem, P. Kara, K. Kerman, B. Meric, J. Hassmann and M. Ozsoz, *Anal. Chem.*, 2002, **74**, 5931-5936.
4. (a) N. Hui, X. Sun, S. Niu and X. Luo, *ACS Appl. Mater. Interfaces*, 2017, **9**, 2914-2923; (b) B. S. Ferguson, S. F. Buchsbaum, J. S. Swensen, K. Hsieh, X. Lou and H. T. Soh, *Anal. Chem.*, 2009, **81**, 6503-6508.
5. (a) P. Wang, H. Wu, Z. Dai and X. Zou, *Chem. Commun.*, 2012, **48**, 10754-10756; (b) E. Farjami, L. Clima, K. V. Gothelf and E. E. Ferapontova, *Analyst*, 2010, **135**, 1443-1448; (c) C. Singhal, C. S. Pundir and J. Narang, *Biosens. Bioelectron.*, 2017, **97**, 75-82; (d) H.-S. Wang, H.-X. Ju and H.-Y. Chen, *Electroanalysis*, 2002, **14**, 1615-1620; (e) H. Aoki and Y. Umezawa, *Electroanalysis*, 2002, **14**, 1405-1410.
6. (a) J. P. Bartolome, L. Echegoyen and A. Fragoso, *Anal. Chem.*, 2015, **87**, 6744-6751; (b) C. C. Mayorga-Martinez, A. Chamorro-Garcia, L. Serrano, L. Rivas, D. Quesada-Gonzalez, L. Altet, O. Francino, A. Sanchez and A. Merkoci, *J. Mater. Chem. B*, 2015, **3**, 5166-5171; (c) M. Freitas, M. Sá Couto, M. F. Barroso, C. Pereira, N. de-los-Santos-Álvarez, A. J. Miranda-Ordieres, M. J. Lobo-Castañón and C. Delerue-Matos, *ACS Sens.*, 2016, **1**, 1044-1053.
7. (a) S. J. Kwon and A. J. Bard, *J. Am. Chem. Soc.*, 2012, **134**, 10777-10779; (b) Kashish, S. Gupta, S. K. Dubey and R. Prakash, *Anal. Methods,*, 2015, **7**, 2616-2622; (c) M. A. Mehrgardi and L. E. Ahangar, *Biosens. Bioelectron.*, 2011, **26**, 4308-4313; (d) H.-F. Cui, T.-B. Xu, Y.-L. Sun, A.-W. Zhou, Y.-H. Cui, W. Liu and J. H. T. Luong, *Anal. Chem.*, 2015, **87**, 1358-1365; (e) J. Liu, M. Tian and Z. Liang, *Electrochim. Acta*, 2013, **113**, 186-193.
8. (a) X. Miao, Z. Li, A. Zhu, Z. Feng, J. Tian and X. Peng, *Biosens. Bioelectron.*, 2016, **83**, 39-44; (b) J. Das and H. Yang, *J. Phys. Chem. C*, 2009, **113**, 6093-6099; (c) T. Zhang, P. Chen, Y. Sun, Y. Xing, Y. Yang, Y. Dong, L. Xu, Z. Yang and D. Liu, *Chem. Commun.*, 2011, **47**, 5774-5776.
9. (a) Z. L. Zhang, D. W. Pang, H. Yuan, R. X. Cai and H. Abruna, *Anal. Bioanal. Chem.*, 2005, **381**, 833-838; (b) S. F. Liu, J. Liu, L. Wang and F. Zhao, *Bioelectrochemistry*, 2010, **79**, 37-42; (c) H. F. Cui, T. B. Xu, Y. L. Sun, A. W. Zhou, Y. H. Cui, W. Liu and J. H. T. Luong, *Anal. Chem.*, 2015, **87**, 1358-1365; (d) G. J. Li, X. L. Li, J. Wan and S. S. Zhang, *Biosens. Bioelectron.*, 2009, **24**, 3281-3287.
10. S. L. Li, W. W. Qiu, X. Zhang, J. C. Ni, F. Gao and Q. X. Wang, *Sens. Actuator B-Chem.*, 2016, **223**, 861-867.
11. (a) I. Grabowska, D. G. Singleton, A. Stachyra, A. Gora-Sochacka, A. Sirko, W. Zagorski-Ostoja, H. Radecka, E. Stulz and J. Radecki, *Chem. Commun.*, 2014, **50**, 4196-4199; (b) A. Brewer, G. Siligardi, C. Neylon and E. Stulz, *Org. Biomol. Chem.*, 2011, **9**, 777-782.
12. T. B. K. C, S. Tada, L. Zhu, T. Uzawa, N. Minagawa, S.-C. Luo, H. Zhao, H.-h. Yu, T. Aigaki and Y. Ito, *Chem. Commun.*, 2018, **54**, 5201-5204.
13. (a) K. Kurzątkowska, A. Sirko, W. Zagórski-Ostoja, W. Dehaen, H. Radecka and J. Radecki, *Anal. Chem.*, 2015, **87**, 9702-9709; (b) K. Malecka, A. Stachyra, A. Góra-Sochacka, A. Sirko, W. Zagórski-Ostoja, W. Dehaen, H. Radecka and J. Radecki, *Biosens. Bioelectron.*, 2015, **65**, 427-434; (c) I. Grabowska, A. Stachyra, A. Góra-Sochacka, A. Sirko, A. B. Olejniczak, Z. J. Leśnikowski, J. Radecki and H. Radecka, *Biosens. Bioelectron.*, 2014, **51**, 170-176.
14. M. P. N. Bui, T. J. Baek and G. H. Seong, *Anal. Bioanal. Chem.*, 2007, **388**, 1185-1190.
15. E. Laviron, *J. Electroanal. Chem. Interfacial Electrochem.*, 1979, **100**, 263-270.
16. (a) C. Macca and J. Wang, *Anal. Chim. Acta*, 1995, **303**, 265-274; (b) Y. Umezawa, K. Umezawa and H. Sato, *Pure Appl. Chem.*, 1995, **67**, 507-518.
17. M. E. Swartz and I. S. Krull, *Handbook of analytical validation*, CRC Press, 2012.

View Article Online
DOI: 10.1039/C8CC05362F

Table of contents entry

Approaching single DNA molecule detection with an ultrasensitive electrochemical genosensor based on gold nanoparticles and Cobalt-porphyrin DNA conjugates

Balwinder Kaur, Kamila Malecka, Domenico A. Cristaldi, Clarissa S. Chay, Iwona Mames, Hanna Radecka, Jerzy Radecki* and Eugen Stulz*

An ultrasensitive genosensor is obtained by using gold nanoparticles and cobalt-porphyrin labelled DNA reporter strands with an attomolar detection limit.